

1 **Spatial-temporal variability of soil moisture: addressing the monitoring at** 2 **the catchment scale**

3

4 Jacopo Dari, Renato Morbidelli¹, Carla Saltalippi

5 Dept. of Civil and Environmental Engineering, University of Perugia, via G. Duranti 93, 06125

6 Perugia, Italy

7

8 Christian Massari, Luca Brocca

9 National Research Council, Research Institute for Geo-Hydrological Protection, via Madonna Alta

10 126, 06128 Perugia, Italy

11

12 **Abstract**

13 Soil moisture plays a fundamental role in the mass and energy balance between the land surface and the
14 atmosphere, making its knowledge essential for several hydrological and climatic applications. The aim of this
15 study is to extend the current knowledge of soil moisture spatial-temporal variability at the catchment scale (up to
16 500 km²). The main implication is to provide guidelines to obtain soil moisture values representative of the mean
17 behaviour at the medium-sized river basin scale, which is useful for remote sensing validation analysis and rainfall-
18 runoff modeling. To this end, 23 measurements campaigns were carried out during a time span of 14 months at 20
19 sites located within the Upper Chiascio River Basin, a catchment with a drainage area of about 460 km² in the
20 Umbria Region (central Italy). The data set allowed the analysis of both soil moisture temporal stability and its
21 dynamics. On the basis of statistical and temporal stability approaches, it was investigated how factors such as
22 climatic regime and geomorphology influence soil moisture behaviour. For the investigated area, the spatial
23 variability of soil moisture was higher in dry periods with respect to wet periods, mainly due to the rainfall pattern
24 characteristics during different periods of the year. Soil moisture values recorded during wet periods showed a
25 better correlation than those recorded during dry periods. The maximum number of required samples, to obtain
26 the mean areal soil moisture with an absolute error of 3% vol/vol, was found equal to 12. The temporal stability
27 analysis showed that during wet periods just one "optimal" measurement point can provide values of soil moisture
28 representative of the catchment-mean behaviour, while during dry periods the number of "optimal" measurement
29 points became equal to two. Therefore, at the adopted spatial scale the use of a single measurement point can lead
30 to significant errors. From the perspective of soil moisture dynamics, the decomposition of the spatial variance
31 showed that the contribution of the time-invariant component (temporal mean of each site) was predominant on
32 respect to the total spatial variance of absolute soil moisture data, for almost the whole observation period. Results
33 provided guidance to optimize soil moisture sampling by performing targeted measurements at a few selected
34 points representative of the catchment-mean behaviour.

¹ Correspondence to: renato.morbidelli@unipg.it

35

36 **Keywords** Soil moisture, Spatial variability, Temporal stability, Catchment scale, In situ measurements

37 **1. Introduction**

38 Soil moisture is of paramount importance for many hydrological processes (Brocca et al.,
39 2017a). Its knowledge is relevant in several fields which include rainfall-runoff partitioning
40 (Blöschl and Sivapalan, 1995; Brocca et al., 2010b; Koster et al., 2010; Mirus and Loague,
41 2013), landslide forecasting (Brocca et al., 2012a), soil nutrient cycling processes (Schjonning
42 et al., 2003), drought monitoring and agriculture (Crow et al., 2012; Champagne et al., 2015).
43 The spatiotemporal variability of soil moisture content raises many challenges to its definition
44 at various scales. Small-scale variations, due to geomorphological characteristics and soil
45 properties, such as the saturated hydraulic conductivity, occur in the spatial range of a few tens
46 of meters and in the temporal range of a few days (Western et al., 2004). Large-scale variations
47 affect very extensive areas, such as whole basins ($>100 \text{ km}^2$), and are also caused by
48 atmospheric forcings.

49 Practically, ground based measurements and remote sensing techniques can be used to
50 characterize at each scale the spatiotemporal variation of soil water content. Ground based
51 measurements such as time domain reflectometry, neutron probes, capacitance probes and
52 gravimetric analyses provide detailed information on the soil moisture values when careful
53 calibration of devices is available (Romano, 2014). However, these techniques are time
54 consuming, very expensive and provide information only in selected points. To overcome this
55 issue, the use of sensors on board of satellite platforms has been spreading over the past few
56 decades (Fang and Lakshmi, 2013; Brocca et al., 2017b). This technology allows to remotely
57 sense various meteorological data, including soil moisture, over large domain but is limited by
58 the low spatial resolution, ranging from 1 km (e.g., Sentinel-1, Bauer-Marschallinger et al.,

59 2018) to 40 km (e.g., SMAP, Entekhabi et al., 2010) and by the inherent bias of the
60 measurement thus requiring an accurate on-site verification prior their use within model and
61 applications. For these reasons, traditional measurement methods are necessary and still widely
62 used. However, given the high costs, an effort is required to identify soil moisture sampling
63 optimization schemes for reducing the number of measurements as few as possible in
64 accordance with the desired accuracy and the site characteristics.

65 Several authors investigated the possibility to optimize the sampling scheme through specific
66 soil moisture field campaigns in experimental areas characterized by dimension up to few
67 square kilometers by using the statistical analysis (Bell et al., 1980; Famiglietti et al., 1999;
68 Brocca et al., 2007; Wang et al., 2008), the temporal stability analysis (Vachaud et al., 1985;
69 Grayson and Western, 1998; Martinez-Fernandez and Ceballos, 2005; Brocca et al., 2009; Zhou
70 et al., 2013), or both (Jacobs et al., 2004; Choi and Jacobs, 2007; Brocca et al., 2010a; Hu et
71 al., 2010; Brocca et al., 2012b; Baroni et al., 2013; Liao et al. 2017; Lai et al., 2017; Lai et al.,
72 2018). Recently, Mittelbach and Seneviratne (2012), considering a very large scale (the entire
73 Switzerland area), showed that the spatial variability of soil moisture is predominantly
74 determined by a time-invariant component and that statistical and temporal stability analysis
75 can lead to different results by considering temporal anomalies rather than absolute soil
76 moisture values. Mittelbach and Seneviratne (2012) concluded their analysis encouraging
77 further studies at different scale to investigate the spatio-temporal characteristics of temporal
78 soil moisture anomalies in addition to assessments of those of absolute soil moisture.

79 All these studies highlighted that soil moisture spatial variability increases with the extension
80 of the investigated area and that soil moisture patterns show a significant temporal stability,
81 thus making just one optimal measurement point able to represent the areal mean behaviour.
82 However, at the catchment scale, for large areas, especially during seasons with strong

83 propensity for the development of convective rainfall systems, as stated in terms of optimal
84 sampling scheme for the small scale could fail.

85 Therefore, the main objective of this paper, aimed at the determination of an optimal soil
86 moisture sampling scheme, is to investigate the soil water content behaviour at a scale in which
87 the rainfall spatial variability may play an important role. For this purpose, the analysis carried
88 out in this paper is based on a long measurement period which has been divided into wet and
89 dry sub-periods in order to explore the influence of convective and frontal rainfall systems on
90 soil moisture variability. At the same spatial scale, on the basis of the methodology proposed
91 by Mittelbach and Seneviratne (2012), the secondary objective of this paper is to evaluate the
92 roles of the time-invariant contribution of the temporal anomalies in the determination of the
93 spatial variability of soil moisture.

94 **2. Materials and Methods**

95 *2.1 Study area*

96 The soil moisture measurements were carried out in 20 experimental sites located in the Upper
97 Chiascio River Basin, which is an inland area in the Umbria Region with a drainage area of
98 approximately 460 km² (Fig. 1). The basin was mainly characterized by an Apennine climate
99 with an altitude between 320 and 1550 m a.s.l. and a mean slope of 24%. The mean annual
100 temperature was 13.0 °C and the mean annual precipitation was 1050 mm, generally with the
101 highest monthly values recorded in the autumn and winter seasons.

102

103 *insert here Fig. 1*

104

105 2.2 Soil moisture measurements

106 The selection of the 20 experimental sites for the monitoring of soil moisture was based on the
107 necessity to have heterogeneity in terms of land use, topography, texture and vegetation cover.
108 With this choice (site number and position) we tried to represent the entire catchment
109 considering also the necessity to conduct each measurement campaign in the same day.

110 As shown in Table 1, the distribution of soil texture classes of the measurement points was
111 fairly uniform with most of the sites located in silty clay loam and clay loam (respectively 30%
112 and 35% of the total) soils. The terrain of the experimental sites was mostly flat, with 70% of
113 the measurement points placed in flat areas and 30% in hilly areas. With regard to land use, the
114 area where the experimental sites are located was predominantly cultivated, with small wooded
115 areas and semi-natural environments. The sampling scheme adopted was designed to have a
116 number of measurement points and measurement campaigns that can catch the soil moisture
117 spatial and temporal variability. In fact, experimental sites were located on an extended area
118 and the measurement campaigns were prolonged to capture the alternation between dry and wet
119 periods. The 23 monitoring campaigns covered a time span ranging from March 2014 to May
120 2015 and were distanced between them for about two weeks each. During each field campaign,
121 four measures were carried out at each of the 20 monitored sites and the mean value was
122 considered as the reference value to be stored in the database. The soil moisture was measured
123 through a portable unit using two wire connector-type Time Domain Reflectometry probes
124 (TDR) of the Soil Moisture Equipment Corporation - TRASE® TDR, which provides a soil
125 moisture measurement representative for a soil layer depth of 15 cm. To obtain the volumetric
126 soil moisture once the dielectric constant is measured, the standard calibration curve was used
127 (Skaling, 1992). The equipment has a quoted error within $\pm 2\%$ vol/vol. Except for the texture
128 classes given in Table 1, a detailed characterization of the study soils is delayed for future
129 developments, which could also highlight further aspects of interest.

130

131 *insert here Table 1*

132

133 *2.3 Rainfall data*

134 The rainfall pattern that affected the study basin during the measurement period was analysed
135 in order to separate dry from wet periods. The daily rainfall data recorded by 14 rain gauges
136 located within the area of interest was collected and spatially averaged by using the Thiessen
137 Polygon method.

138

139 *2.4 Statistical analysis*

140 The main statistical features of the soil moisture data set were determined and analysed in terms
141 of spatial and temporal variability.

142 Let us denote θ_{ij} the soil moisture measured at site i ($i = 1, \dots, N$) during the sampling day j ($j =$
143 $1, \dots, M$), with $N = 20$ and $M = 23$; the spatial mean referred to each sampling day, $\bar{\theta}_j$, is given
144 by:

$$145 \quad \bar{\theta}_j = \frac{1}{N} \sum_{i=1}^N \theta_{ij} \quad (1)$$

146 in a similar way, the temporal mean for each measurement point, $\bar{\theta}_i$, is calculated by:

$$147 \quad \bar{\theta}_i = \frac{1}{M} \sum_{j=1}^M \theta_{ij} \quad (2)$$

148 The coefficient of variation for each sampling day, CV_j , is obtained from the relation:

$$149 \quad CV_j = \frac{\sigma_j}{\bar{\theta}_j} = \frac{\sqrt{\frac{1}{N-1} \sum_{i=1}^N (\theta_{ij} - \bar{\theta}_j)^2}}{\bar{\theta}_j} \quad (3)$$

150 where σ_j is the “spatial” standard deviation. For each site, the coefficient of variation in time,
151 CV_i , and the temporal standard deviation, σ_i , can be defined analogously.

152 The number of required samples for estimating the mean value within a specific absolute error,
153 NRS, can be obtained from the knowledge of σ_j through the following implicit relation (Wang
154 et al., 2008):

$$155 \quad NRS = t_{1-\frac{\alpha}{2}, NRS}^2 \left(\frac{\sigma_j^2}{AE^2} \right) \quad (4)$$

156 where $t_{1-\frac{\alpha}{2}, NRS-1}^2$ is the value of the Student’s t-distribution at the confidence level $1-\alpha/2$, NRS
157 is the number of the degrees of freedom and AE indicates the absolute error considered,
158 expressed in volumetric soil moisture (% vol/vol).

159

160 *2.5 Temporal stability*

161 The temporal stability analysis, introduced by Vauchad et al. (1985), allows to identify the
162 measurement points where the observed values of soil moisture are representative of the mean
163 soil moisture of the entire monitored area. This is extremely important because it permits to
164 install a small number of probes in a few selected points for retrieving the average soil moisture
165 over a large area. Furthermore, the knowledge of the temporal persistence of soil moisture
166 patterns provides support in determining the frequency of measurements under different
167 wetness conditions. The temporal stability analysis is carried out using the relative differences
168 method, which is described below. Considering the spatial mean for each sampling day
169 previously introduced, the relative difference, δ_{ij} , referring to site i and sampling day j is
170 calculated by:

$$171 \quad \delta_{ij} = \frac{(\theta_{ij} - \bar{\theta}_j)}{\bar{\theta}_j} \quad (5)$$

172 For each measurement point i , the mean, $\bar{\delta}_i$, and the standard deviation, $\sigma(\delta_i)$, of the relative
173 differences can be obtained by:

$$174 \quad \bar{\delta}_i = \frac{1}{M} \sum_{j=1}^M \delta_{ij} \quad (6)$$

$$175 \quad \sigma(\delta_i) = \sqrt{\frac{1}{M-1} \sum_{j=1}^M (\delta_{ij} - \bar{\delta}_i)^2} \quad (7)$$

176 The $\bar{\delta}_i$ quantifies how much the soil moisture recorded at a sampling point departs from the
177 mean spatial value during the measurement period; the $\sigma(\delta_i)$ is an index of the temporal
178 variability. The “representative” sites of the mean value in time are characterized by lower
179 values of $|\bar{\delta}_i|$ and $\sigma(\delta_i)$.

180 Jacobs et al. (2004) defined a single metric to identify the best sampling point, the index of time
181 stability, ITS, that combines the $\bar{\delta}_i$ and its $\sigma(\delta_i)$. It can be calculated, for each site, as follows:

$$182 \quad ITS_i = [\bar{\delta}_i^2 + \sigma(\delta_i)^2]^{1/2} \quad (8)$$

183 It is noteworthy that originally in Jacobs et al. (2004) this index was called root mean square
184 error (RMSE). In this study, the wording ITS (Zhao et al., 2010; Penna et al., 2013) is employed
185 instead of RMSE in order to disambiguate the index of time stability from the common
186 definition of the RMSE. According to this method, “optimal” measurement points are
187 characterized by low values of the ITS; the main advantage of the ITS approach is that it allows
188 to identify representative sampling sites by considering just one parameter.

189

190 *2.6 Decomposition of soil moisture spatial variance*

191 The soil moisture dynamics were studied on the basis of the approach introduced by Mittelbach
192 and Seneviratne (2012). According to this method, the spatial variance of soil moisture data can
193 be decomposed in the following three components:

$$194 \quad \sigma^2(\theta_{ij}) = \sigma^2(\bar{\theta}_i) + \sigma^2(A_{ij}) + 2\text{cov}(\bar{\theta}_i, A_{ij}) \quad (9)$$

195 where $\sigma^2(\bar{\theta}_i)$ is the spatial variance of the temporal mean, $\sigma^2(A_{ij})$ is the spatial variance of the
196 temporal anomalies, A_{ij} , which quantify how much each observed value deviates from the
197 temporal mean and can be calculated as:

$$198 \quad A_{ij} = \theta_{ij} - \bar{\theta}_i \quad (10)$$

199 The third component of the right side in Eq. (8) is the spatial covariance between the temporal
200 mean soil moisture of a site and the temporal anomaly.

201

202 *2.7 Data processing*

203 The observed data were analysed both in their completeness and by considering partial sets
204 based on temporal and spatial criteria. Specifically, the values of soil moisture recorded during
205 wet and dry periods were compared, as well as those observed in flat and hilly areas. The
206 separation between dry and wet periods was determined by analysing the rainfall measurements
207 occurred in the experimental area in the measurement period. For each day in which a
208 measurement campaign was carried out, it was calculated the mean of the daily rainfall recorded
209 by 14 rain gauges installed thereabout the experimental sites. This operation was repeated for
210 the five days previous each measurement campaign; the spatial averages were then summed
211 obtaining the values of API5 referred to each sampling day. The periods in which these values
212 were found higher than a mean threshold value were classified as “wet”, otherwise as “dry”.

213

214 **3. Results**

215

216 *3.1 Statistical analysis*

217 The time series of soil moisture values observed at each site, their spatial mean and the average
218 rainfall over the study area during the measurement period are shown in Fig. 2; the spatial mean
219 soil moisture responds to the precipitation input with sudden increments after significant events
220 and slow decrements in the absence of precipitation. Two wet and two dry periods have been
221 identified in the time interval of interest.

222

223 *insert here Fig. 2*

224

225 The spatial mean, the spatial standard deviation and the coefficient of variation of the soil
226 moisture obtained during each measurement campaign are contained in Table 2. It also shows
227 the associated value of API5 (the average value considering 14 rain gauges) and its coefficient
228 of variation, CV API5. The behaviour of the CV API5 values reported in Table 2 evidences the
229 different rainfall patterns during the various periods of the year. In presence of prevailing
230 convective systems, mainly observed during dry periods, the average CV API5 is equal to 1.03,
231 while with prevailing frontal systems, typically observed during wet periods, this value become
232 0.63.

233

234 *insert here Table 2*

235

236 As expected, for both soil moisture and API5, the values of the coefficient of variation of the
237 soil moisture obtained during each measurement campaign were lower during the wet periods.
238 In fact, during the dry season, the average CV_j of soil moisture was equal to 0.21, while for the
239 wet season it was equal to 0.16. Globally, i.e. by considering the entire data set, the average
240 value of CV_j was equal to 0.19. This is an index of the low variability of soil moisture field
241 during the wet periods, when the investigated area is interested by spatially uniform rainfall

242 systems; during the dry period, instead, the soil moisture field is less uniform, as a response to
243 isolated convective rainfall systems, that determine significant spatial differences in the soil
244 moisture values.

245 The decreasing trend between CV_j and $\bar{\theta}_j$ is shown in Fig. 3. This behaviour indicates a lower
246 variability of absolute soil moisture under increasing wetness conditions and it is consistent
247 with the behaviour observed in most of the previous analogous studies (e.g., Bell et al., 1980;
248 Famiglietti et al., 1999, 2008; Brocca et al., 2010a; Brocca et al., 2012b) conducted in smaller
249 areas.

250

251 *insert here Fig. 3*

252

253 The assumption that the relationship between CV_j and $\bar{\theta}_j$ is represented by an exponential law
254 allows to establish the maximum NRS for estimating the mean soil moisture value with a
255 specific absolute error (AE) as a function of the average wetness conditions. By using Eq. (4),
256 the NRS values were calculated for an AE equal to 3% and 4% (see Fig. 4). By assuming the
257 relation between CV_j and $\bar{\theta}_j$ as exponential, Eq. 4 provides NRS as a function of the mean soil
258 moisture within a certain level of confidence. For instance, by considering a confidence interval
259 of 95%, to obtain the average soil moisture with an AE of 3%, a maximum NRS of 12 was
260 required. This value was found for a mean soil moisture of ~30% vol/vol and was the maximum
261 of the curve shown in Fig. 4, obtained by fitting the values calculated with Eq. 4 by considering
262 the entire set of soil moisture measurements.

263

264 *insert here Fig. 4*

265

266 Brocca et al. (2012b), on the basis of soil moisture data recorded during a time span of about
267 one year over two areas with a smaller extension (178 and 242 km²) but comparable to those of
268 interest in this study, found a maximum NRS value up to 3 (AE=4%). Obviously, with the
269 increase of the AE, the NRS decreases, reaching the value of 7 for absolute an error of 4%. This
270 method allows to plan a reliable in situ monitoring with respect to a fixed accuracy, also at a
271 catchment spatial scale.

272

273 *3.2 Temporal stability analysis*

274 In order to check out which sites are the most suitable to obtain the benchmark soil moisture,
275 i.e. the areal mean calculated considering all the 20 sites, the relative differences method was
276 applied. For this purpose, the values of $\bar{\delta}_i$, $\sigma(\delta_i)$ and ITS were considered and compared. The
277 application of the ITS method to values of $\bar{\delta}_i$ and $\sigma(\delta_i)$ that vary in ranges quite different from
278 each other could provide unreliable results if the aim is to identify a measurement point
279 temporally stable and representative of the mean soil moisture for the entire study area. Without
280 any standardisation, it could happen that an experimental site shows a low value of ITS because
281 of a low value of $\sigma(\delta_i)$ but a relatively high value of $\bar{\delta}_i$, thus making that point temporally stable
282 but distant from the areal mean soil moisture. In this case, the recorded values should be scaled
283 in order to obtain the areal mean. Because of this, the identification of “optimal” measurement
284 point was here addressed by comparing temporal stability analysis with correlation analysis,
285 always keeping in mind that the final aim is to identify temporally stable sites that could also
286 provide a soil moisture value representative of the catchment-mean behaviour. This procedure
287 was applied for the entire data set and considering the partition between wet and dry periods,
288 in order to highlight the influence of climate conditions on soil moisture variability.
289 Distinguishing between values observed in flat areas from those in hilly areas, it was also

290 possible to evaluate the geomorphological characteristics that experimental sites should have
291 to be considered as optimal measurement sites.

292 The most representative site of the entire study basin, in terms of mean soil moisture, was the
293 number 8 of Fig. 1. Fig. 5a shows the good determination coefficient (R^2 equal to 0.837)
294 between the values found at site 8 and the areal mean soil moisture. Fig. 6a shows the rank
295 ordered mean relative difference, with the corresponding standard deviation, for each
296 experimental site; on the same chart, also the ITS associated to each measurement point is
297 shown. Site 8 showed good characteristics in terms of temporal stability as $|\bar{\delta}_i|$ was close to
298 zero and $\sigma(\delta_i)$, represented by the vertical bar, was very low. The ITS values were minimal for
299 sites 8 and 1, but the latter showed a significant value of $|\bar{\delta}_i|$.

300 By considering the entire data set, the values of $\sigma(\delta_i)$ varied between a minimum and a
301 maximum of 7.6% and 19.7% (in absolute value), respectively. In particular, for the site number
302 8, values of $|\bar{\delta}_i| = 0.003$, $\sigma(\delta_i) = \pm 9.7\%$ and ITS = 9% were found.

303

304 *insert here Fig. 5*

305 *insert here Fig. 6*

306

307 The same analyses were also carried out separately during wet and dry periods, and results are
308 shown in Figs. 5b-c and 6b-c. In the dry periods, the site where the soil moisture values were
309 closer to the average of the study basin was the number 16, with R^2 equal to 0.725 (Fig. 5b),
310 which also showed good characteristics in terms of temporal stability, i.e., low values of $|\bar{\delta}_i|$,
311 $\sigma(\delta_i)$ and ITS, even if these values are worse than those relative to sites 8 and 1. Conversely,
312 during the wet periods, the site 8 was the optimal one, with R^2 equal to 0.857 (Fig. 5c) and the
313 lowest values of $|\bar{\delta}_i|$, $\sigma(\delta_i)$ and ITS. While there is no doubt that during the wet periods the site

314 8 was the “optimal” one, for the dry periods further evaluations are needed; together with site
315 8, site 16 could be chosen as “optimal” for this period because it showed the best determination
316 coefficient with the spatial mean and consequently a $|\bar{\delta}_i|$ closer to zero. For this site the ITS
317 wasn’t the lowest one because of a $\sigma(\delta_i)$ higher than other sites (i.e., site 1). This is probably
318 due to a few values recorded during the transition periods, when the catchment is not yet in
319 uniform wetness conditions. It can be observed that both sites 8 and 16 were located in flat
320 areas. Also if not statistically significant, this interesting indication could be the object of future
321 developments.

322 In the spatial correlation triangle shown in Fig. 7, the generic box identified by the i-th line and
323 j-th column expresses the correlation between the values of soil moisture measured during the
324 i-th campaign and those measured in the j-th campaign. Higher correlations are represented
325 with darker cells. It can be seen that the values of soil moisture measured during campaigns
326 carried out in wet periods were highly correlated each other, while lower values were obtained
327 between campaigns carried out during dry periods. Relatively high correlations were also
328 observed between measurement campaigns belonging to wet periods distant in time (about 5
329 months). The spatial correlation between measurements carried out during wet periods reached
330 values of 0.94 and always remained larger than 0.71. Another aspect of interest was that, in
331 accordance with previous studies (Mohanty and Skaggs, 2001; Cosh et al., 2004; Martinez-
332 Fernandez and Ceballos, 2005; Brocca et al., 2012b), in most cases measurements campaigns
333 during the transition periods were those that show the lower correlation values. Finally,
334 campaigns taken during different dry seasons were occasionally negatively correlated with each
335 other. These results provided useful information for optimize a soil moisture monitoring. For
336 instance, with the objective to validate soil moisture estimation from remote sensing, transition
337 periods should be avoided or, alternatively, an adequate number of sampling points should be
338 adopted.

339

340 *insert here Fig. 7*

341

342 The same analysis was carried out with data separated by site geomorphology. Measurements
343 in flat sites provided values of soil moisture positively correlated with each other over time and
344 significantly higher than those observed in hilly sites, where the correlation was high solely
345 between adjacent measurement campaigns (see Fig. 8). During the wet periods, there was an
346 increase in the spatial correlation between the average soil moisture over hilly areas and the
347 areal mean value; the same happened with the average water content over flat areas.

348

349 *insert here Fig. 8*

350

351 *3.3 Decomposition of soil moisture spatial variance*

352 The analyses previously described, aimed to identify the most representative sites of the mean-
353 catchment soil moisture behaviour, were carried out in terms of absolute values of soil moisture.
354 However, some studies (e.g., Mittelbach and Seneviratne, 2012; Brocca et al., 2014) suggested
355 that the temporal anomalies (the absolute soil moisture minus the seasonal mean) can show a
356 different behaviour with respect to the absolute values. On the basis of this new perspective,
357 Fig. 9 shows the time evolution of the terms that contribute to the determination of spatial
358 variance of soil moisture according to Equation 9. In most cases the dominant contribution was
359 the one related to the temporal mean. The influence of temporal anomalies was higher during
360 dry periods and in some cases larger than that related to the temporal mean. These results were
361 in line with what previously mentioned about the lower stability of soil moisture values
362 observed during the dry season. During the wet periods, the contribution of the covariance was
363 often close to zero, while the time-invariant term was dominant.

364

365 *insert here Fig. 9*

366

367

368 **4. Discussion**

369 *4.1 Statistical and temporal stability analyses*

370 The combination of statistical and temporal stability analysis allowed us to highlight that, also
371 at the large scale (up to 500 km²), soil moisture field showed temporal stability properties. In
372 fact, considering the whole data set, soil moisture measurements in site 8 represented the areal
373 mean with R² equal to 0.837 and RMSE equal to 2.4% vol/vol. During the wet periods, the
374 performances of the same experimental site rose, with a higher determination coefficient and a
375 smaller root mean square error (R² equal to 0.857 and RMSE equal to 1.2% vol/vol). During
376 the dry periods, there was a loss in the accuracy of the estimation. The mean of the values
377 recorded in the “optimal” measurement points (sites 8 and 16) for this period was able to
378 reproduce the catchment-mean behaviour with R² equal to 0.846 and RMSE equal to 1.6%
379 vol/vol. Considering a third experimental site during the dry periods, no significant advantage
380 was gained. In fact, involving also the measurements detected in site 1, that showed good
381 temporal stability properties, the areal mean was reproduced without an increase in R² and with
382 a restrained decrease in the RMSE, reaching the value of 1.2% vol/vol. These results allow us
383 to affirm that a single "optimal" measurement point should be enough during the wet periods,
384 while during the dry periods a couple of selected sites could be necessary. In order to optimize
385 the soil moisture monitoring over the investigated area, not only the number and the location of
386 “optimal” measurement points, but also the frequency of sampling, is of paramount. The lower

387 variability of soil moisture during the wet periods suggests that during wet seasons the sampling
388 can be addressed less frequently than in dry and transition (between dry to wet and vice versa)
389 periods, when the lower temporal persistence of the soil moisture field makes necessary to
390 sample more frequently. This result is in accordance with previous studies (Zhao et al., 2010).
391 The lower correlation obtained during the dry periods and thus the “lower” temporal stability
392 was also confirmed by $\sigma(\delta_i)$ observed in the two periods: it ranged between 3.6% and 12.6%
393 during the wet periods and between 8.1% and 23% during the dry ones.

394 At the scale considered in this paper, climatic factors address the soil moisture behaviour in the
395 same way for different morphological conditions. In fact, soil moisture values recorded in flat
396 sites were more correlated with the areal mean than those found in hilly areas, both for the dry
397 and wet seasons. Although the different number of flat and hilly sites may influence this result,
398 it is equally true that a drainage slower than in the inclined slopes associated with the absence
399 of horizontal fluxes may explain this phenomenon, making this morphologic feature relevant
400 for the identification of optimal measurement points, especially at the catchment scale
401 considered in this paper, characterized by high possibility to find a variable geomorphology.

402 Finally, we remark that the magnitude of CV_j values was in agreement with results obtained in
403 previous studies characterized by similar conditions (Famiglietti et al., 1999; Western and
404 Blöschl, 1999). More specifically, a comparison with studies conducted in central Italy (Brocca
405 et al., 2007, 2009, 2010a, 2012b) showed how the average value of CV_j increases with the size
406 of the investigated area, assuming values equal to: (i) 0.06-0.08 at local scale (1-500 m²), (ii)
407 0.10 at small plot scale (501-5000 m²), (iii) \approx 0.15 at plot scale (5001-100,000 m²) and (iv) \approx
408 0.20 at small catchment scale (50-240 km²). In this work, the experimental area was larger than
409 those examined in the above-mentioned studies, and the heterogeneity of topography and land
410 use was more significant. Therefore, we expect to find a higher value of CV_j that however is
411 consistent (\sim 0.20) with the values observed for areas equal to 240 km². Consequently, at least

412 in central Italy, it might be assumed that the average value of CV_j equal to ~ 0.20 represents an
413 upper limit of the expected spatial variability of soil moisture observations. This result is very
414 important when a distributed rainfall-runoff model has to be used.

415

416 *4.2 Decomposition of soil moisture spatial variance*

417 Considering the entire measurement period, in accordance with Mittlebach and Seneviratne
418 (2012) and Brocca et al. (2014), the component due to the temporal mean provided the highest
419 contribution (61%) to the total variance, also if the spatial variability of temporal anomalies can
420 never be neglected. During the wet periods the landscape and soil characteristics such as texture
421 and land cover exert a large influence on the soil moisture spatial distribution, larger than the
422 contribute related to the climatic factors which mainly impact the anomaly term. This can be
423 also associated to the type of precipitation systems that affect the Mediterranean area which are
424 synoptic during the winter season and more convective all through the summer. During the
425 transition periods, the gap between the contribution of the temporal mean and of the anomalies
426 decreased in favour of the latter as also demonstrated in a recent study (see i.e. Gao et al., 2015)
427 and the climatic factors become significant likely due the alternation of warm and cold days
428 determined by weather variability. During the summer months (June, July and August) the
429 contributions of temporal mean and anomalies reached the maximum annual values with first
430 still dominating the second but less than during the wet season. This result reinforces what
431 previously mentioned about the analysis of the correlation between the measurement campaigns
432 in relation to the lower reliability of soil moisture surveys carried out during the dry and
433 especially transient periods. Moreover, another important aspect to be considered for the
434 analysis of the time-variant and time-invariant component is the spatial scale. Results depends
435 on the spatial heterogeneities of time-invariant components such as soil texture and vegetation
436 that are expected to be less variable at smaller spatial scale. In this study, we have performed

437 the analysis at basin scale, 500 km², that is much smaller than the region investigated in
438 Mittlebach and Seneviratne (2012), 31500 km², and much larger than those considered in Gao
439 et al. (2015), 0.6 km². As expected, we have obtained that the time-invariant component is less
440 (more) important than in Mittlebach and Seneviratne (2012) (Gao et al., 2015), with results
441 similar to those found in Brocca et al. (2014) who analysed different networks at different
442 spatial scales.

443

444 **5. Conclusions**

445 Soil moisture measurements carried out in 20 experimental sites in the Upper Chiascio River
446 Basin for a period longer than one year have been used to investigate the soil moisture behaviour
447 at a spatial scale (~500 km²) in which the rainfall spatial variability may play an important role.
448 Based on results obtained from statistical and temporal stability analyses, as well as from the
449 decomposition of the soil moisture spatial variance, the following conclusions can be drawn:

- 450 1. The maximum number of required samples (NRS), considering an absolute error (AE)
451 of 3% vol/vol and intermediate wetness conditions, is equal to 12.
- 452 2. Soil moisture exhibits greater variability during dry and transition periods. In fact, the
453 average coefficient of variation for the dry season is equal to 0.21, while for the wet one
454 it is equal to 0.16.
- 455 3. Also for areas up to 500 km², the soil moisture field exhibits temporal stability. More
456 specifically, during wet periods, one “optimal” measurement site allows estimating the
457 areal mean value with a good agreement ($R^2 = 0.857$ and $RMSE = 1.2\%$ vol/vol), while
458 during dry periods a couple of representative sites becomes necessary. In this way, the
459 catchment-mean pattern is reproduced with $R^2 = 0.846$ and $RMSE = 1.6\%$ vol/vol. The
460 most representative sites are located over flat areas. This last result, distinctive of the

461 large scale adopted in this paper, is mainly due to the rainfall pattern characteristics
462 during different periods of the year.

463 4. The total spatial variance of absolute soil moisture data is predominantly determined by
464 the time-invariant component, due to the temporal mean of each site. However, during
465 the summer season and the transition periods, the gap between the contribution of the
466 temporal mean and of the anomalies significantly decreases.

467

468 These results represent a useful support to optimize any soil moisture sampling over areas with
469 dimension up to 500 km². Further analyses, aimed to investigate deeper layers or to assess the
470 effects of different land uses and soil properties on the spatiotemporal variability of soil
471 moisture in the study basin, are still needed.

472

473 **Acknowledgment**

474 This work was partially funded by the Italian Ministry of Education, University and Research (MIUR), within the
475 project ‘Experimental Hydrological Database for Apennine Basins’ (DIBA, Database Idrologico Bacini
476 Appenninici), developed in the context of the program *Nextdata*.
477

478 **References**

479 Baroni, G., Ortuani, B., Facchi, A., Gandolfi, C., 2013. The role of vegetation and soil
480 properties on the spatio-temporal variability of the surface soil moisture in a maize cropped
481 field. *Journal of Hydrology*, 489, 148-159.

482 Bauer-Marschallinger, B., Naeimi, V., Cao, S., Paulik, C., Schaufler, S., Stachl, T., Modanesi,
483 S., Ciabatta, L., Massari, C., Brocca, L., Wagner, W., 2018. Towards global soil moisture
484 monitoring with Sentinel-1: harnessing assets and overcoming obstacles. submitted to *IEEE*
485 *Transactions on Geoscience and Remote Sensing*.

486 Bell, K. R., Blanchard, B. J., Schmutge, T. J., Witzczak, M. W., 1980. Analysis of surface
487 moisture variations within large field sites. *Water Resources Research*, 16, 796-810.

488 Blöschl, G., Sivaplan, M., 1995. Scale issues in hydrological modelling: a review. *Hydrological*
489 *Processes*, 9, 251-290.

490 Brocca, L., Ciabatta, L., Massari, C., Camici, S., Tarpanelli, A., 2017a. Soil moisture for
491 hydrological applications: open questions and new opportunities. *Water*, 9(2), 140.

492 Brocca, L., Crow, W.T., Ciabatta, L., Massari, C., de Rosnay, P., Enenkel, M., Hahn, S.,
493 Amarnath, G., Camici, S., Tarpanelli, A., Wagner, W., 2017b. A review of the applications of
494 ASCAT soil moisture products. *IEEE Journal of Selected Topics in Applied Earth Observations
495 and Remote Sensing*, 10(5), 2285-2306.

496 Brocca, L., Melone, F., Moramarco, T., Morbidelli, R., 2009. Soil moisture temporal stability
497 over experimental areas of central Italy. *Geoderma*, 148 (3-4), 364-374.

498 Brocca, L., Melone, F., Moramarco, T., Morbidelli, R., 2010a. Spatial-temporal variability of
499 soil moisture and its estimation across scales. *Water Resources Research*, 46, W02516.

500 Brocca, L., Melone, F., Moramarco, T., Wagner, W., Naeimi, V., Bartalis, Z., Hasenauer, S.,
501 2010b. Improving runoff prediction through the assimilation of the ASCAT soil moisture
502 product. *Hydrology and Earth System Sciences*, 14, 1881-1893.

503 Brocca, L., Morbidelli, R., Melone, F., Moramarco, T., 2007. Soil moisture spatial variability
504 in experimental areas of central Italy. *Journal of Hydrology*, 333, 356-373.

505 Brocca, L., Ponziani, F., Moramarco, T., Melone, F., Berni, N., Wagner, W., 2012a. Improving
506 Landslide Forecasting Using ASCAT-Derived Soil Moisture Data: A Case Study of the
507 Torgiovanetto Landslide in Central Italy. *Remote sensing*, 4(5), 1232-1244.

508 Brocca, L., Tullo, T., Melone, F., Moramarco, T., Morbidelli, R., 2012b. Catchment scale soil
509 moisture spatial-temporal variability. *Journal of Hydrology*, 422-423, 63-75.

510 Brocca, L., Zucco, G., Mittelbach, H., Moramarco, T., Seneviratne, S. I., 2014. Absolute versus
511 temporal anomaly and percent of saturation soil moisture spatial variability for six networks
512 worldwide. *Water Resources Research*, 50, 2014WR015684.

513 Champagne, C., Davidson, A., Cherneski, P., L'Heureux, J., Hawden, T., 2015. Monitoring
514 agricultural risk in Canada using L-band passive microwave soil moisture from SMOS. *Journal
515 of Hydrometeorology*, 16, 5-18.

516 Choi, M., Jacobs, J. M., 2007. Soil moisture variability of root zone profile within SMEX02
517 remote sensing footprints. *Advances in Water Resources*, 30 (4), 883-896.

518 Cosh, M. H., Stedinger, J. R., Brutsaert, W., 2004. Variability of soil moisture at the watershed
519 scale. *Water Resources Research*, 40 (12), W12513.

520 Crow, W. T., Kumar, S. V., Bolten, J. D., 2012. On the utility of land surface models for
521 agricultural drought monitoring. *Hydrology and Earth System Sciences*, 16, 3451-3460.

522 Entekhabi, D., Njoku, E.G., Neill, P.E., Kellogg, K.H., Crow, W.T., Edelstein, W.N., et al.,
523 2010. The soil moisture active passive (SMAP) mission. *Proceedings of the IEEE*, 98(5), 704-
524 716.

525 Famiglietti, J. S., Deveraux, J. A., Laymon, C. A., Tsegaye, T., Houser, P. R., Jackson, T. J.,
526 Graham, S. T., Rodell, M., van Oevelen, P. J., 1999. Ground-based investigation of soil

527 moisture variability within remote sensing footprints during the Southern Great Plains 1997
528 (SGP97) hydrology experiment. *Water Resources Research*, 35(6), 1839-1851.

529 Famiglietti, J. S., Ryu, D., Berg, A. A., Rodell, M., Jackson, T. J., 2008. Field observations of
530 soil moisture variability across scales. *Water Resources Research*, 44, 16, W01423.

531 Fang, B., Lakshmi, V., 2013. Soil moisture at watershed scale: Remote sensing techniques.
532 *Journal of Hydrology*, 516, 258-272.

533 Gao, X., Zhao, X., Si, B. C., Brocca, L., Hu, W., Wu, P., 2015. Catchment-scale variability of
534 absolute versus temporal anomaly soil moisture: Time-invariant part not always plays the
535 leading role. *Journal of Hydrology*, 529, 1669-1678.

536 Grayson, R. B., Western, A. W., 1998. Towards areal estimation of soil water content from
537 point measurements: time and space stability of mean response. *Journal of Hydrology*, 207, 68-
538 82.

539 Hu, W., Shao, M.A., Han, F., Reichardt, K., Tan, J., 2010. Watershed scale temporal stability
540 of soil water content. *Geoderma*, 158, 181-198.

541 Jacobs, J. M., Mohanty, B. P., En-Ching, H., Miller, D., 2004. SMEX02: field scale variability,
542 time stability and similarity of soil moisture. *Remote Sensing of Environment*, 92, 436-446.

543 Koster, R. D., Mahanama, S. P. P., Livneh, B., Lettenmaier, D. P., Reichle, R. H., 2010. Skill
544 in streamflow forecasts derived from large-scale estimates of soil moisture and snow. *Natural*
545 *Geoscience*, 3, 613-616.

546 Lai, X., Zhu, Q., Zhou, Z., Liao, K., 2017. Influences of sampling size and pattern on the
547 uncertainty of correlation estimation between soil water content and its influencing factors.
548 *Journal of Hydrology*, 555, 41-50.

549 Lai, X., Zhou, Z., Zhu, Q., Liao, K., 2018. Identifying representative sites to simultaneously
550 predict hillslope surface and subsurface mean soil water contents. *Catena*, 167, 363-372.

551 Liao, K., Zhou, Z., Lai, X., Zhu, Q., Feng, H., 2017. Evaluation of different approaches for
552 identifying optimal sites to predict mean hillslope soil moisture content. *Journal of Hydrology*,
553 547, 10-20.

554 Martinez-Fernandez, J., Ceballos, A., 2005. Mean soil moisture estimation using temporal
555 stability analysis. *Journal of Hydrology*, 312, 28-38.

556 Mittelbach, H., Seneviratne, S. I., 2012. A new perspective on the spatio-temporal variability
557 of soil moisture: temporal dynamics versus time-invariant contributions. *Hydrology and Earth*
558 *System Sciences*, 16, 2169-2179.

559 Mirus, B. B., Loague, K., 2013. How runoff begins (and ends): Characterizing hydrologic
560 response at the catchment scale. *Water Resources Research*, 49, 2987-3006.

561 Mohanty, B. P., Skaggs, T. H., 2001. Spatio-temporal evolution and time-stable characteristics
562 of soil moisture within remote sensing footprints with varying soil, slope, and vegetation.
563 *Advances in Water Resources*, 24 (9-10), 1051-1067.

564 Penna, D., Brocca, L., Borga, M., Dalla Fontana, G., 2013. Soil moisture temporal stability at
565 different depths on two alpine hillslopes during wet and dry periods. *Journal of Hydrology*, 477,
566 55-71.

567 Romano, N., 2014. Soil moisture at local scale: measurements and simulations. *Journal of*
568 *Hydrology*, 516, 6-20.

569 Schjonning, P., Thomsen, I.K., Moldrup, P., Christensen, B.T., 2003. Linking soil microbial
570 activity to water- and air-phase contents and diffusivities. *Soil Science Society of American*
571 *Journal*, 67, 156-165.

572 Skaling, W., 1992. TRASE: a product history. In: Topp, G. C. (Ed.), *Advances in*
573 *Measurements of Soil Physical Properties: Bridging Theory and Practice*. Soil Science Society
574 of America Journal. Madison, Wis. pp. 169-185.

575 Vauchad, G., Passerat de Silans, A., Balabanis, P., Vauclin, M., 1985. Temporal stability of
576 spatial measured soil water probability density function. *Soil Science Society of America*
577 *Journal*, 49, 822-828.

578 Wang, C., Zuo, Q., Zhang, R., 2008. Estimating the necessary sampling size of surface soil
579 moisture at different scales using a random combination method. *Journal of Hydrology*, 352 (3-
580 4), 309-321.

581 Western, A. W., Blöschl, G., 1999. On the spatial scaling of soil moisture. *Journal of*
582 *Hydrology*, 217, 203-224.

583 Western, A. W., Zhou, S. L., Grayson, R. B., McMahon, T. A., Blöschl, G., Wilson, D. J., 2004.
584 Spatial correlation of soil moisture in small catchments and its relationship to dominant spatial
585 hydrological processes. *Journal of Hydrology*, 286, 113-134.

586 Zhao, Y., Peth, S., Wang, X. Y., Lin, H., Horn, R., 2010. Controls of surface soil moisture
587 spatial patterns and their temporal stability in a semi-arid steppe. *Hydrological Processes*, 24,
588 2507-2519.

589 Zhou, J., Fu, B. J., Lü, N., Gao, G. Y., Lü, Y. H., Wang, S., 2013. Temporal stability of soil
590 moisture under different land uses/cover in the Loess Plateau based on a finer spatiotemporal
591 scale. *Hydrology and Earth System Sciences Discussion*, 10, 10083-10125.

592
593
594
595
596

597 **List of Tables**

598

599 **Table 1** Soil texture (according to the USDA classification), land use, terrain and altitude of the 20
600 selected measurement points (a.s.l.: above sea level).

601

602 **Table 2** Statistic parameters (mean, $\bar{\theta}_j$, standard deviation, σ_j , and coefficient of variation, $CV_j(\theta)$) of
603 the observed soil moisture and average values of API5 calculated for each sampling day, considering 14
604 rain gauges, with the corresponding coefficient of variation, CV API5.

605

606

607

608

609 **Figure captions**

610

611 **Fig. 1** Chiascio River Basin: location of the experimental sites for soil moisture monitoring.

612

613 **Fig. 2** Time series of soil moisture observed on each experimental site with the mean rainfall precipitated
614 during the entire measurement period. The bold line indicates the time series of the spatial mean of soil
615 moisture referring to the whole area under examination.

616

617 **Fig. 3** Decreasing trend of the coefficient of variation as the average soil moisture increases. The chart
618 also reports the exponential interpolating law.

619

620 **Fig. 4** Number of soil moisture samples required (NRS) to capture the catchment-mean soil moisture
621 considering a confidence interval of 95% for various absolute errors (AE). The fitting was made in
622 accordance with Eq. 4 considering the soil moisture dataset and varying the AE.

623

624 **Fig. 5** Comparison of the areal mean soil moisture versus the soil moisture observed at the most
625 representative sites (the numbers 8 and 16 of Fig. 1) considering: a) the entire data set, b) the dry periods
626 and c) the wet periods.

627

628 **Fig. 6** Rank ordered mean relative difference for a) the entire data set, b) dry periods, c) wet periods.
629 Labels indicate measurement sites (see also Fig. 1) and the vertical bars indicate standard deviation.

630

631 **Fig. 7** Correlation matrix of the observed soil moisture values during the measurement campaigns.

632

633 **Fig. 8** Correlation matrices of the observed soil moisture values in a) flat sides and b) hilly sites.

634

635 **Fig. 9** Time series of contributions determining spatial variance of soil moisture and their sum for the
636 entire reference period, in accordance with equation (9), expressed as a percentage of the total. The
637 green is the contribution of temporal mean, the red that related to temporal anomalies, that is time-
638 dependent, such as the contribution of covariance between the previous two (blue). The black represents
639 the total spatial variance.

640

641

642
643
644
645
646

Table 1 Soil texture (according to the USDA classification), land use, terrain and altitude of the 20 selected measurement points (a.s.l.: above sea level).

<i>Site</i>	<i>Soil texture</i>	<i>Land use</i>	<i>Terrain</i>	<i>Altitude (m a.s.l.)</i>
1	Silty clay loam	Agricultural	Flat	380
2	Silty clay loam	Agricultural	Flat	405
3	Silty clay loam	Agricultural	Flat	436
4	Silty clay loam	Agricultural	Flat	457
5	Loam	Agricultural	Flat	452
6	Clay loam	Agricultural	Flat	428
7	Loam	Agricultural	Flat	436
8	Silt loam	Agricultural	Flat	396
9	Clay loam	Forest and semi-natural	Hilly	453
10	Clay	Forest and semi-natural	Hilly	380
11	Silt loam	Forest and semi-natural	Hilly	408
12	Silty clay loam	Agricultural	Flat	400
13	Silt loam	Forest and semi-natural	Flat	409
14	Clay loam	Agricultural	Flat	497
15	Clay loam	Agricultural	Flat	431
16	Clay loam	Artificial surfaces	Flat	459
17	Silty clay loam	Agricultural	Flat	422
18	Clay loam	Agricultural	Hilly	553
19	Loam	Agricultural	Hilly	575
20	Clay loam	Forest and semi-natural	Hilly	624

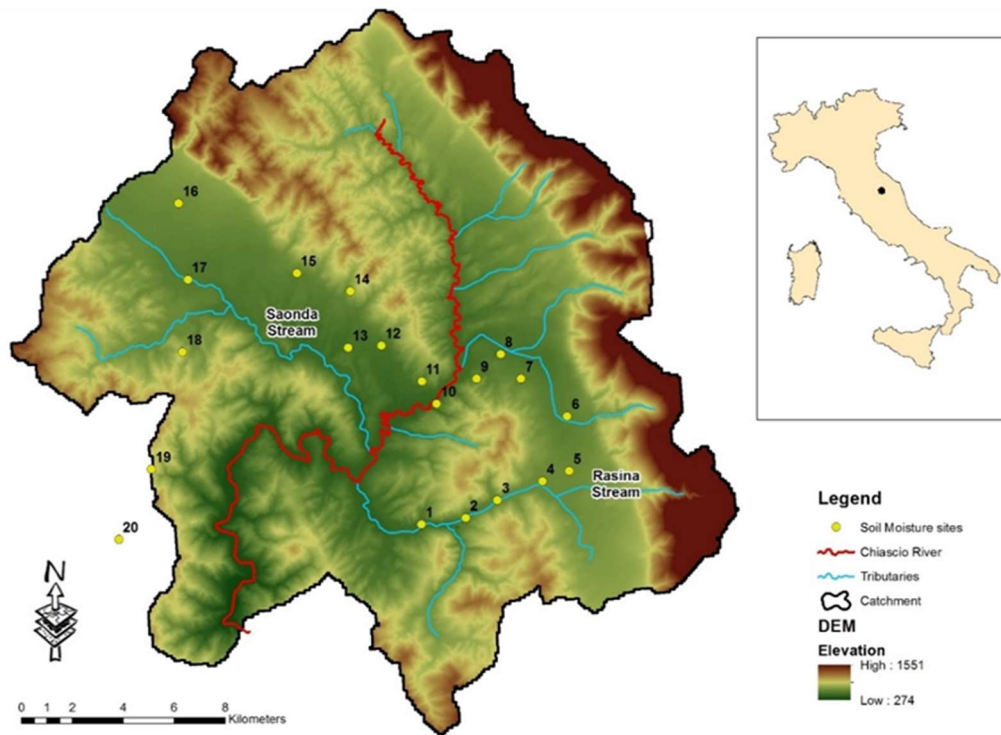
647
648

649
 650
 651
 652
 653
 654

Table 2 Statistic parameters (mean, $\bar{\theta}_j$, standard deviation, σ_j , and coefficient of variation, $CV_j(\theta)$) of the observed soil moisture and average values of API5 calculated for each sampling day, considering 14 rain gauges, with the corresponding coefficient of variation, CV API5.

	<i>Date - (progressive number)</i>	$\bar{\theta}_j$ (%)	σ_j (%)	$CV_j(\theta)$	<i>API5 [mm]</i>	<i>CV API5</i>
<i>Wet</i>	26/03/14 - (1)	33.09	5.44	0.16	20.60	0.48
	14/04/14 - (2)	32.84	5.26	0.16	15.61	0.57
	08/05/14 - (3)	32.71	4.96	0.15	21.96	0.26
<i>Dry</i>	04/06/14 - (4)	26.92	6.20	0.23	10.23	0.70
	20/06/14 - (5)	25.84	5.25	0.20	37.28	1.63
	02/07/14 - (6)	25.07	4.20	0.17	14.14	0.19
	06/08/14 - (7)	30.34	3.95	0.13	11.58	0.77
	20/08/14 - (8)	20.65	5.49	0.27	0.04	1.61
	09/09/14 - (9)	24.15	5.53	0.23	0.15	1.08
	24/09/14 - (10)	25.81	3.89	0.15	5.12	0.91
	09/10/14 - (11)	21.16	5.46	0.26	0.08	1.11
	23/10/14 - (12)	24.72	4.75	0.19	3.33	0.53
	04/11/14 - (13)	25.09	5.43	0.22	0.04	1.43
<i>Wet</i>	21/11/14 - (14)	33.94	5.28	0.16	83.48	0.22
	05/12/14 - (15)	36.42	5.02	0.14	29.98	0.26
	18/12/14 - (16)	37.06	4.83	0.13	12.17	0.37
	28/01/15 - (17)	36.29	5.78	0.16	9.16	0.77
	11/02/15 - (18)	35.78	5.08	0.14	17.23	0.36
	10/03/15 - (19)	36.67	6.80	0.19	25.72	0.43
	24/03/15 - (20)	35.11	6.84	0.19	1.82	2.57
<i>Dry</i>	13/04/15 - (21)	25.71	5.56	0.22	0.00	-
	08/05/15 - (22)	21.05	5.79	0.27	0.00	2.09
	29/05/15 - (23)	29.12	4.84	0.17	8.67	0.38

655
 656



658
659
660
661

Fig. 1 Chiascio River Basin: location of the experimental sites for soil moisture monitoring.

662

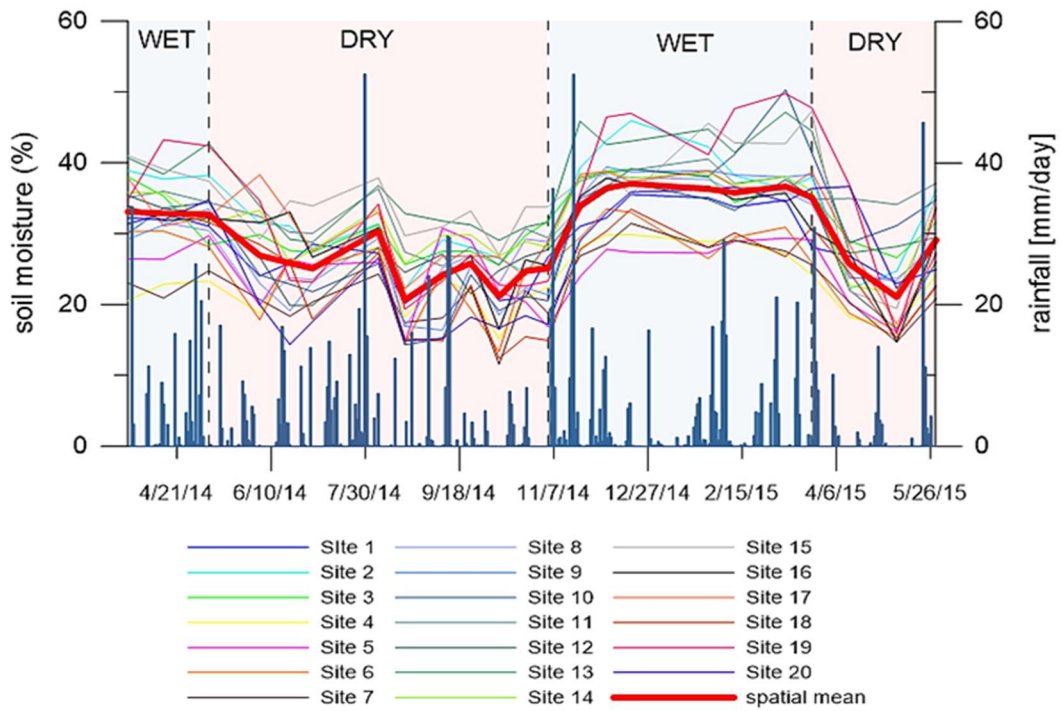
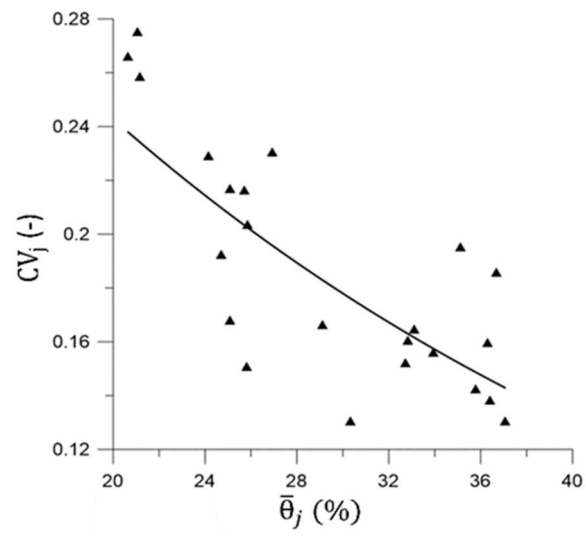


Fig. 2 Time series of soil moisture observed on each experimental site with the mean rainfall precipitated during the entire measurement period. The bold line indicates the time series of the spatial mean of soil moisture referring to the whole area under examination.

668



669

670

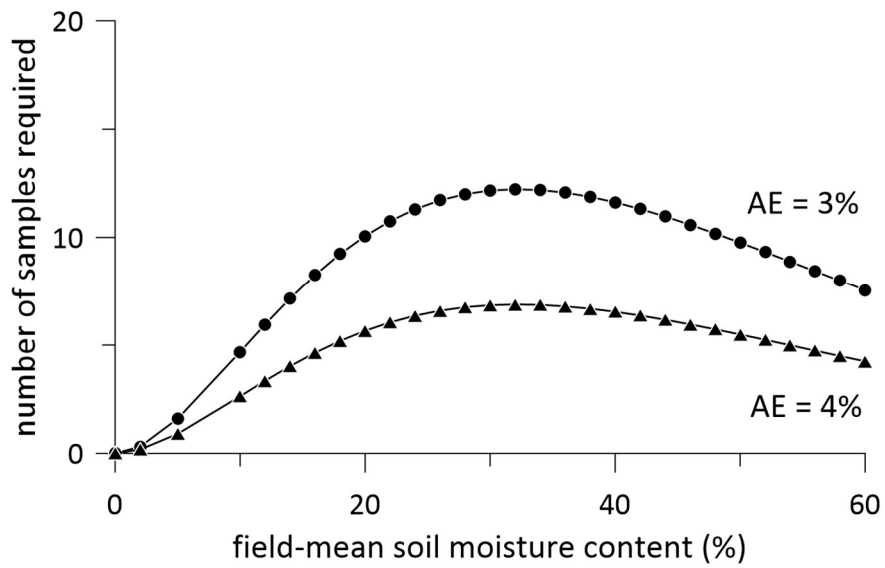
671 **Fig. 3** Decreasing trend of the coefficient of variation of the observed soil moisture as the average soil

672 moisture increases. The chart also reports the exponential interpolating law.

673

674

675



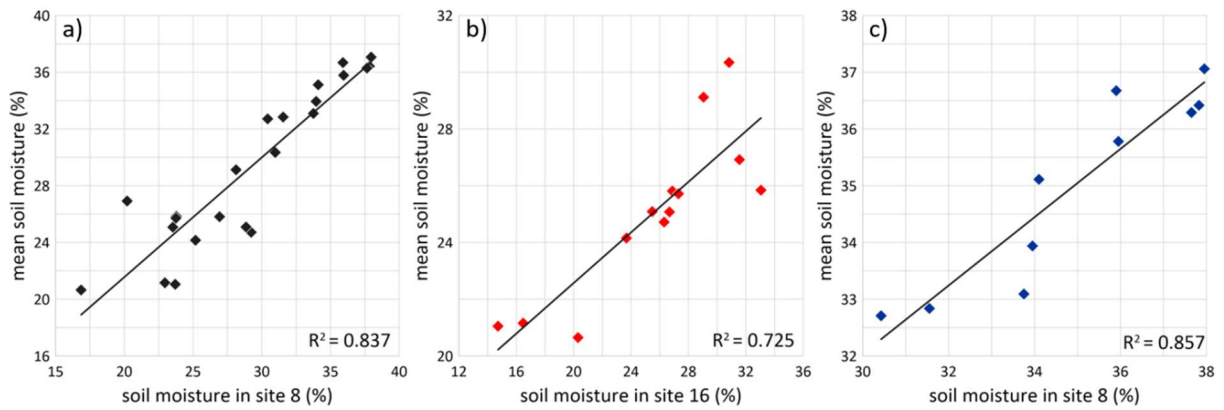
676

677

678 **Fig. 4** Number of soil moisture samples required (NRS) to capture the catchment-mean soil moisture
679 considering a confidence interval of 95% for various absolute errors (AE). The fitting was made in
680 accordance with Eq. 4 considering the soil moisture dataset and varying the AE.

681

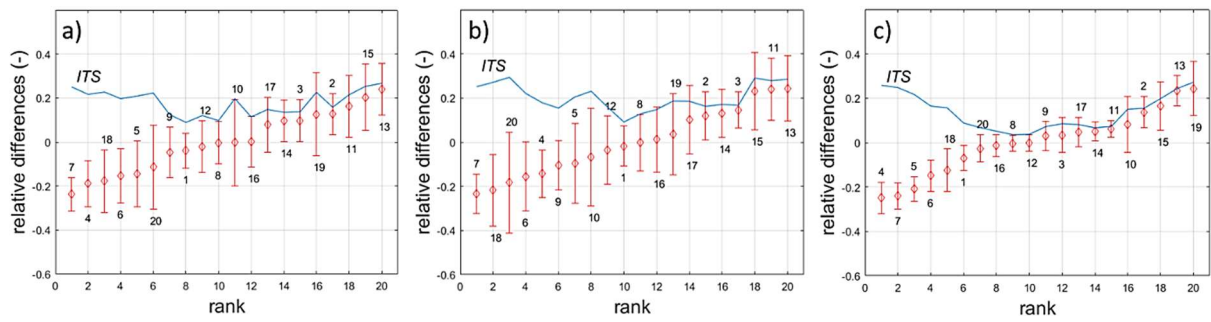
682
683
684



685
686
687
688
689
690
691

Fig. 5 Comparison of the areal mean soil moisture versus the soil moisture observed at the most representative sites (the numbers 8 and 16 of Fig. 1) considering: a) the entire data set, b) the dry periods and c) the wet periods.

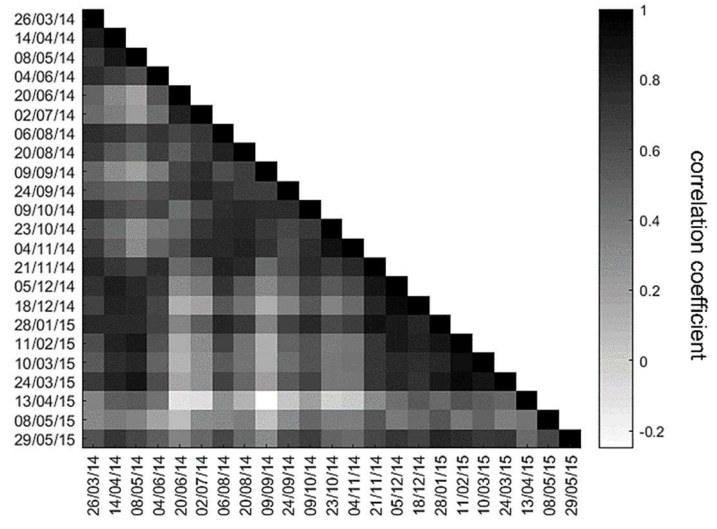
692
693
694



695
696
697
698
699
700

Fig. 6 Rank ordered mean relative difference and the ITS for a) the entire data set, b) dry periods, c) wet periods. Labels indicate measurement sites (see also Fig. 1) and the vertical bars indicate standard deviation.

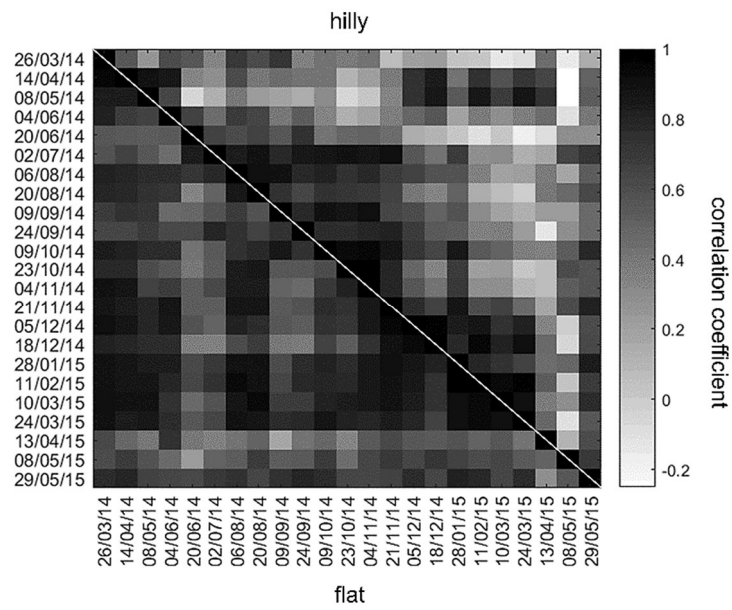
701
702



703
704
705
706

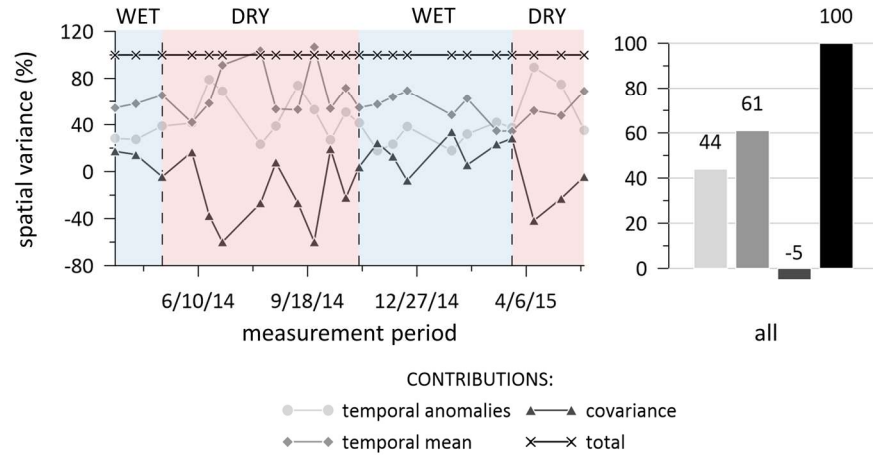
Fig. 7 Correlation triangle of the observed soil moisture values during the measurement campaigns.

707
708



709
710
711
712
713

Fig. 8 Correlation matrix of the observed soil moisture values in flat (under the diagonal) and hilly (above the diagonal) sites.



715
 716
 717
 718
 719

Fig. 9 Time series of contributions determining spatial variance of soil moisture and their sum for the entire reference period, in accordance with equation (9), expressed as a percentage of the total.